Journal of Structural Geology 32 (2010) 1279–1290

Contents lists available at ScienceDirect

Journal of Structural Geology

journal homepage: www.elsevier.com/locate/jsg

Evolution of anastomosing crack–seal vein networks in limestones: Insight from an exhumed high-pressure cell, Jabal Shams, Oman Mountains

Marc Holland*,[1], Janos L. Urai

Structural Geology Tectonics Geomechanics, RWTH Aachen University, Lochnerstrasse 4-20, D-52066 Aachen, Germany

ARTICLE INFO

Article history:
Received 12 January 2008
Received in revised form
12 August 2008
Accepted 9 April 2009
Available online 5 May 2009

Keywords:
Zebra carbonate
Crack–seal
Anastomosing
Veins

ABSTRACT

We studied a special type of zebra carbonate in limestones of an overpressure cell exhumed from at 5 km depth, in outcrops on Jabal Shams, Oman Mountains. The rocks show anastomosing patterns of regularly spaced calcite veins in dark gray, fine-grained carbonate; microscopic observations reveal these as dense bundles of much finer veinlets, typically 10–50 μm thick. The vein bundles are up to 5 mm thick, they contain multiple sub-parallel arrays of host rock fragments embedded in the coarse-grained vein calcite. We interpret these structures as the result of numerous mechanically effective crack and reseal events together with strong growth competition or crystallization from sparse nucleation sites. Cementation produced mechanically strong veins so that new fractures were localized along the vein/rock interface or within the matrix itself. We present simple conceptional models relating the mechanical strength of the vein and the morphology of the resulting vein network.

1. Introduction

In this study we discuss the formation of brightly colored, thin calcite veins in a dark carbonate matrix. Such a macroscopic texture is commonly described by the term "zebra-rock", which can be produced by a number of different processes, such as primary sedimentation, metasomatosis as well as different means of fracturing (e.g. Badoux et al., 2001; Merino et al., 2006; Nielsen et al., 1998, 2000; Swennen et al., 2003; Vandeginste et al., 2005; Weller, 1989). In the context of these different possibilities, the study of the micro-structural properties not only reveals the processes responsible for forming the texture, but also allows deriving the genetic conditions. Accessing these parameters is important in order to decide whether the presented zebra texture has the potential to be used as indicative information.

Over a range of scales, the texture of our samples is made up of an extremely dense network of anastomosing veins, which we interpret to have formed by crack–seal processes (Andreani et al., 2004; Boullier and Robert, 1992; Gaviglio, 1986; Hilgers and Urai, 2005; Lee and Wiltschko, 2000; Petit et al., 1999; Ramsay, 1980; Renard et al., 2005; Wiltschko and Morse, 2001). The exceptional high density of healed fractures, and the corresponding pattern, raises questions on how this special form of zebra pattern was formed. We attempt to explain the genetic conditions and present simple conceptual models that discuss the role of cementation in restoring the rock strength.

2. Description

2.1. Geological framework

The samples of this study were collected on the southern flank of Jabal Shams in the Oman Mountains. The Oman Mountains are part of the Alpine–Himalayan chain and show a complex multiphase deformation (e.g. Al-Wardi, 2006; Al-Wardi and Butler, 2006; El-Shazly et al., 2001; Glennie, 2005; Hilgers et al., 2006; Holland et al., 2009; Loosveld et al., 1996; Searle, 2007) of which details like the strain portioning, timing and tectonic framework are still unclear (e.g. Breton et al., 2004; Gray et al., 2005a,b; Gray and Miller, 2000; Searle, 2007; Searle et al., 2005; Warren and Miller, 2007; Warren et al., 2003; Wilson, 2000). The area exposes carbonates and mudstones that belong to the 'Autochthonous' Hajar Supergroup. The rocks of this group were deposited in a predominantly passive margin environment (Glennie, 2005; Hughes Clarke, 1988; Searle, 2007). The autochthonous group was subject to a multiphase deformation related to the convergence of the Arabian with the Eurasian plate. This first led to a flexure of the lithosphere causing local uplift of the Arabian plate margin (El-Shazly et al., 2001; Filbrandt et al., 2006; Loosveld et al., 1996; Patton and O'Conner, 1988; Searle, 2007; Warbuton et al., 1990).

* Corresponding author. Fax: +49 2418092358.
E-mail address: mholland@geomi.com (M. Holland).
URL: http://www.ged.rwth-aachen.de
[1] Present address: GeoMechanics International Inc., Emmerich Josef-Str. 5, D-55116 Mainz, Germany.

0191-8141/$ – see front matter © 2009 Elsevier Ltd. All rights reserved.
doi:10.1016/j.jsg.2009.04.011

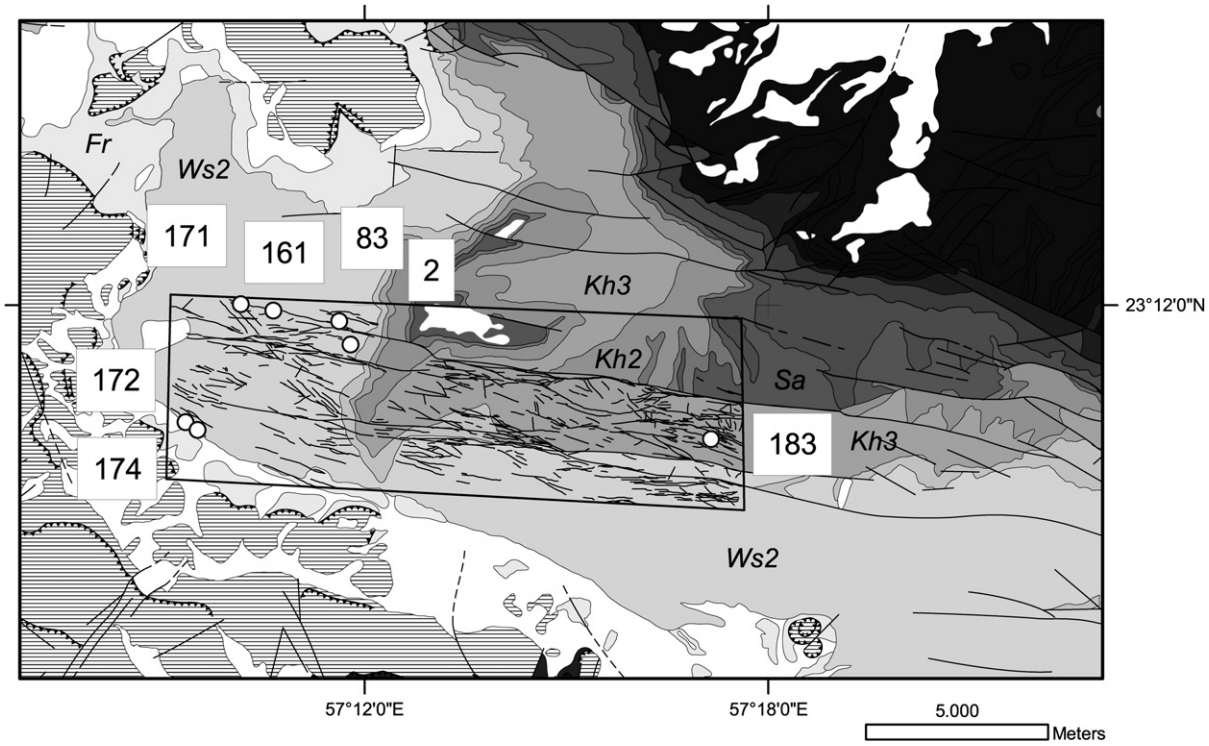

Fig. 1. Location of the outcrops of the zebra patterns on the southern slope of Jabal Shams. Interpreted faults and sample sites are superimposed on a geological map (Ws = Wasia Grp; Kh = Kahmah Grp; Lined sections are nappe units; Box indicates section interpreted, WGS-84 map datum). Changed after Beurrier et al. (1986).

With ongoing convergence two large nappe units were emplaced onto the Arabian plate margin. The load of the Hawasina and the Semail Ophiolite nappes (Campanian and Maastrichtian) reversed the trend and buried the Hajar Supergoup to several kilometers depth (Breton et al., 2004; Glennie, 2005; Hilgers et al., 2006; Holland et al., 2009).

The nappe emplacement stopped with the subduction of the buoyant lithosphere, leading to a time of tectonic quiescence. The large wavelength folds of the Oman Mountains and the exhumation of the rocks are the result of a more recent phase that started in the Tertiary, continuing until today caused by the ongoing convergence of the Eurasian and Arabian plates (Breton et al., 2004; Glennie, 2005; Kusky et al., 2005). The metamorphic gradient in the exposed rocks decreases towards the Southwest with Anchizone conditions in the area of Jabal Shams (Breton et al., 2004).

This multiphase orogenesis caused the formation of several generations of fractures and faults that are all cemented with calcite and minor quartz (Hilgers et al., 2006; Holland et al., in press, 2009). Hilgers et al. (2006) studied veins in the Jabal Akhdar anticline, established overprinting relationships, and reported stable isotope analyses of the cements. These authors concluded that the first generations of vein-filled fractures were created in a rock-buffered environment with fluid pressures close to lithostatic.

Holland et al. (in press, 2009) studied veins in the SW of the Jebel Akhdar anticline, near Oman's highest peak Jabal Shams. They showed that these first generation veins can be further divided into at least four sets of bedding-perpendicular veins.

These four sets show no signs of mechanical interaction; abutting of veins is absent and Holland et al. proposed that the fractures were consistently cemented prior to the formation of new ones.

These first generation bedding-perpendicular veins were overprinted by two more generations of veins. First- by second-generation veins formed in bedding-parallel shear zones. Hilgers et al. (2006) interpret these to have also formed in a rock-buffered environment with pressures close to lithostatic conditions. The isotopic signature of the calcite cement changes in the third generation of veins, that are associated with dilatant normal faults (Hilgers et al., 2006). Their isotopic signature shows evidence of meteoric fluids, suggesting that the normal faults drained the system, which is described as a high-pressure cell (Al-Wardi, 2006; Hilgers et al., 2006; Holland et al., 2009).

2.2. Outcrops

The zebra textures presented in this study are found in outcrops of the Kahmah and Wasia groups exposed near Jabal Shams in the Oman Mountains. The metamorphic conditions of the area correspond to the anchizone with the onset of pressure solution and the evolution of cleavage in phyllosilicate-rich lithologies (Breton et al., 2004). The zebra veins are found in carbonate mudstones and wackstones at different stratigraphic positions. These veins are oriented normal to the bedding, and are therefore interpreted to be part of the first generation veins. The zebra textures are occasionally overprinted by other veins of this group including fractures with shear components. Although cross-cutting relationships with the other veins are evident no abutting is present. Outcrops with zebra veins are not common, the pattern of their occurrence is not yet clear. We note however, that the seven outcrops we studied are also located within a few tens of meters from the later (third generation) normal fault zones (Holland et al., 2009) (Fig. 1). Apart from the spatial context no direct signs for interaction or interconnection of faults and zebra veins were observed.

In some cases the thick (up to 10 cm) veins grade laterally into zebras as the thick veins bifurcate into the sub-parallel strands of the zebra texture. The zebra vein network may either fade into intact rock or form a transition zone towards another massive fist generation vein (Figs. 2 and 3A, D). When the interconnected veins are not aligned, the zebra veins in between commonly show curved trajectories.

The patches of zebra veins are typically in the order of a few centimeters to several 10s of centimeters wide. The bands of bright veins in the pattern are sub-parallel or show a braided pattern causing an irregular macroscopic appearance (Figs. 2 and 3A, B).

2.3. Samples

Samples with zebra textures were collected from the outcrops for micro-structural and geochemical analyses. The samples were cut perpendicular to the veins and polished. After drying, the specimens were stained with an Alizarin and potassium ferricyanide III solution to show iron content and Ca- vs. Mg-content (Adams and MacKenzie, 2001; Kraus, 2002a,b). The stained samples show pink to brown colors indicating non-ferroan calcite. No evidence for pervasive dolomitization or other means of zonation is present among the stained samples (Fig. 4). Thin sections were made for micro-structural analysis and cathodoluminescence (CL). However none of the samples showed CL zonation. Stable carbon and oxygen isotope data were collected from different generation veins and from the rock matrix. The few data points from the zebra veins show an isotope signature similar to that of the surrounding matrix (Table 1).

The pattern of the zebra veins changes with the scale of observation. Down to a 0.1 mm scale, sub-parallel or braided veins are apparent. At larger magnifications, the pattern of the vein network shows a clear increase in complexity (Fig. 5). The macroscopic veins are locally made up of bundles of much smaller veins. The smallest are in the order of 10–25 μm, for which we will use the term "veinlet", whereas we call bundled veinlets or thicker elements "veins".

To describe the complex vein pattern on a thin section scale, a box-counting algorithm is applied. A threshold filter that maximized the optical contrast was used to produce a binary image on which the algorithm counts the amount of boxes containing vein elements using different box sizes. Between the scales of 10 mm and 10 μm, the box-counting shows a power-law relationship (Fig. 6) (Walsh and Watterson, 1993).

The thick veins of the network are approximately 5 mm wide and are macroscopically visible. The thin sections show that the thick veins invariably splay into branches with large variation both in width and shape forming undulating and sometimes angular morphologies (Fig. 5). The smallest veinlets have apertures in the order of 10–25 μm, defining the lower limit of the self-similar pattern. Observations on isolated veinlets within the matrix show them to be trans-granular. Cross-cutting is seldom observed, whereas abutting at a high angle is absent among the veins and veinlets.

The thick veins show sub-parallel arrays of wall rock inclusions, giving them a laminated appearance (Fig. 7). Branching of vein arrays, or isolated veinlets, from the thick bundles is apparent (Figs. 5 and 7). When segments of isolated veins form an oblique angle to a bundle they show curve shapes towards the contact. The veinlets thus merge with the bundles rather than abutting or cross-cutting them.

The calcite cement of the vein network is made of blocky calcite grains with occasional twinning. Fibrous calcite is absent. In thicker vein sections, there is no evidence for growth competition normal to the fracture walls as the grain boundaries are approximately normal to wall (Hilgers et al., 2001; Nollet et al., 2005; Urai et al., 1991). We found no evidence for grain boundary migration recrystallization (Urai et al., 1991).

The individual veinlets consist of calcite grains that stretch from wall to wall. The length of the grains parallel to the walls is several times the width of the veinlet (Fig. 8A). In braided sections, the calcite grains commonly extend into the different branches (Fig. 8B) or across the parallel stacks of the solid inclusions.

Fig. 2. Irregular vein segment showing host rock flakes incorporated at different sections. The lower part of the vein shows how the massive fracture splits into numerous fine veins. Location 174.

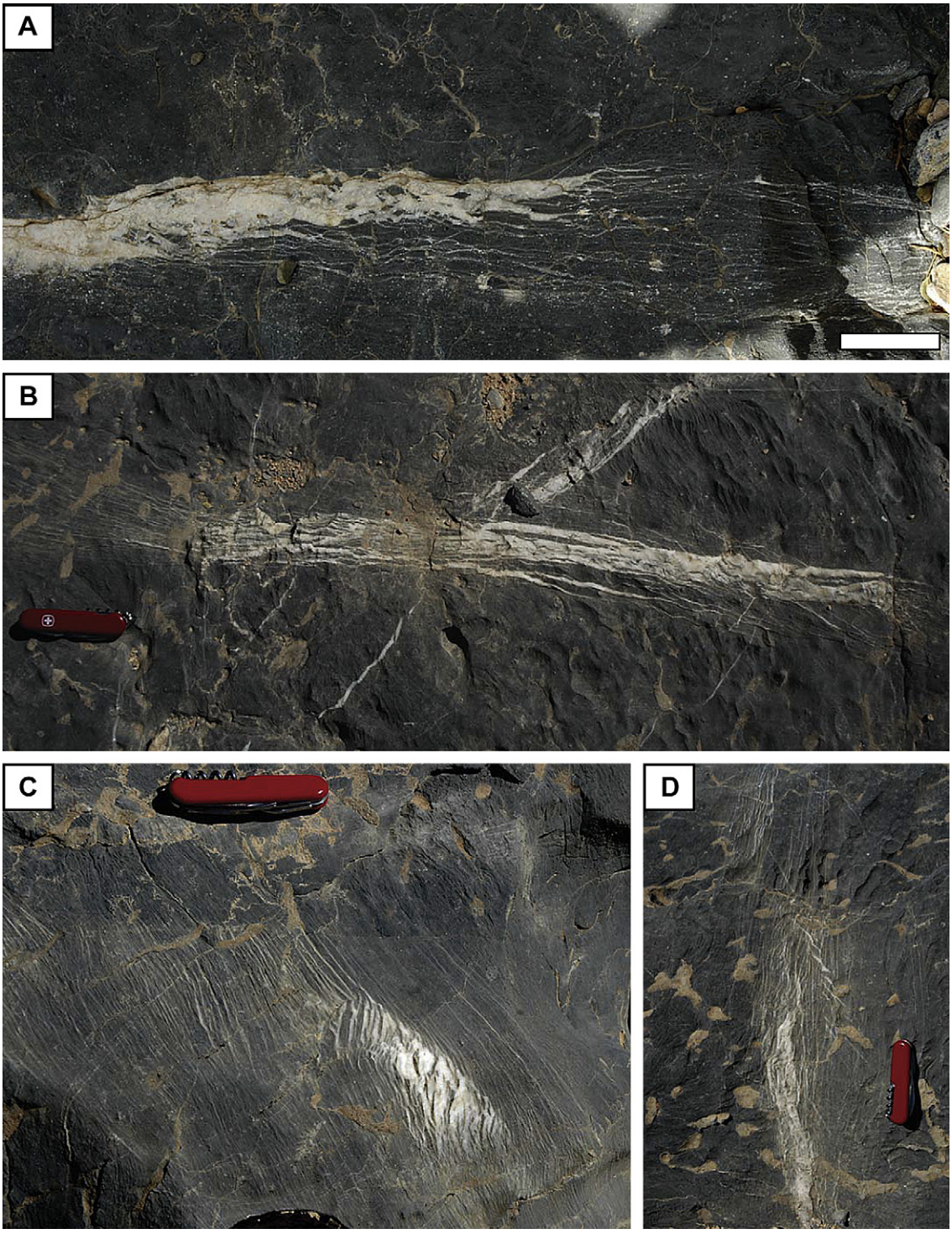

Fig. 3. Macroscopic photographs of zebra textures identified in the field. (A) Massive vein that terminates with numerous fine veins branching off. Scale bar is approx. 1 cm; Location 174. (B) Isolated irregular vein segment made of a dense network of smaller veins; these taper into the host rock. Location 83. (C) Isolated pull-apart vein segment associated with a dense zebra texture. Location 83. (D) Vein termination into numerous vein segments. Location 83.

3. Interpretation

In this study we investigated a texture of densely spaced calcite veins within a dark carbonate rock. The zebra pattern consists of thin veinlets branching and merging, with abundant elongated host rock or solid inclusions. Only the massive bundles are macroscopically visible (Figs. 4C and 5).

Although found close to normal faults (Fig. 1), a genetic relation of the zebra veins to the faults is unclear and we interpret these structures as belonging to the first set of bedding-perpendicular veins in the area. The stable isotope values of the zebra veins are similar to those of the adjacent wall rock (Table 1).

The trajectory of individual veinlets merging with a vein bundle is shown by the arrangement of the solid inclusions separating the

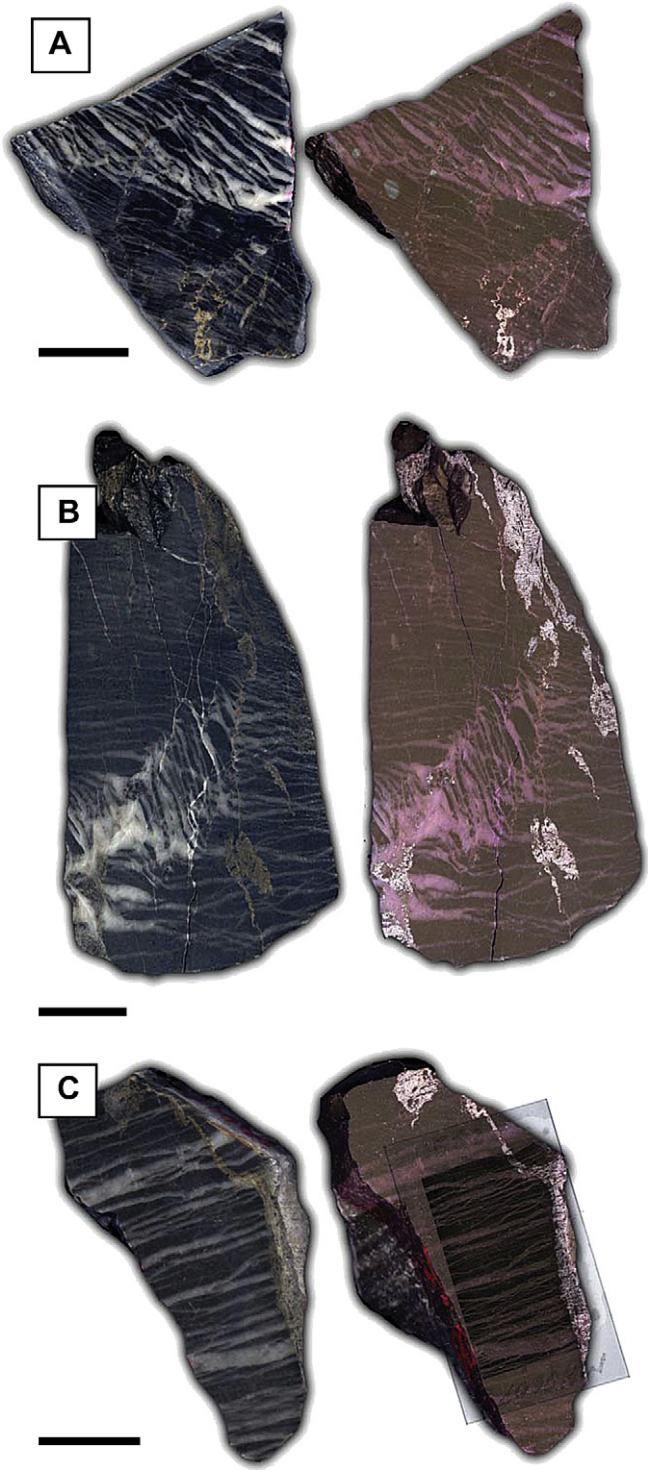

Fig. 4. Scanned samples prior and after staining with Alizarin and potassium ferricyanide III dilution. The moistened samples illustrate the variety of differently sized veins. The staining shows a homogenous coloring of pink to brownish colors indicating non-ferroan calcite material (all samples from Location 83; scale bars are all 2 cm wide).

veinlets within the bundle (Fig. 7). These lensoid matrix fragments form sub-parallel discontinuous bands with a regular spacing. This extremely dense (supersaturated) fracture network could not have been formed in a single "catastrophic" event. Because in this case, the matrix fragments would have settled and accumulated at the bottom. We interpret that the dense anastomosing network formed during a repeated series of crack–seal events, which determined

Table 1
Stable isotope data of matrix and the zebra veins. The values are similar, as shown by the isotope ratios of vein/matrix in the last two columns. This indicates a rock-buffered system.

Specimen	Description	$\delta^{13}C$ [PDB]	$\delta^{18}O$ [VSMOW]	$\delta^{13}C_V/\delta^{13}C_M$	$\delta^{18}O_V/\delta^{18}O_M$
w02	matrix	3.61	25.95		
w02	n3 vein	3.79	25.98	1.05	1.00
w02	s2 vein	3.82	25.96	1.06	1.00
vein	s2 vein	2.59	27.89		
w01	matrix	3.87	26.11		
w01	v1 vein (coarse)	3.90	26.29	1.01	1.01
w01	v1 vein (fine)	3.89	26.22	1.01	1.00
w03a	matrix	1.72	25.92		
w03a	n3 vein (infill)	1.20	27.04	0.70	1.04
w03a	n3 vein	1.91	26.13	1.11	1.01
0607	**zebra vein**	**3.36**	**26.09**	**0.93**	**1.01**
0607	**zebra matrix**	**3.62**	**25.76**		
0610	s2 vein	3.22	28.67		
0610	v1 vein	−0.16	27.58		
0611	v3 vein	3.25	25.85		
e08	n3 vein	2.67	26.26	1.04	0.98
e08	matrix	2.58	26.72		
e02	s2 vein	3.54	27.32	1.02	1.02
e02	matrix	3.49	26.88		
0607	**zebra vein**	**3.34**	**26.07**	**0.92**[a]	**1.01**[a]
0607	**zebra vein**	**3.35**	**26.03**	**0.93**[a]	**1.01**[a]
w03b	n3 vein	1.78	26.87		
w03b	n3 vein (infill)	0.87	27.37		
e01	n3 vein	3.24	26.45		
e015	n3 vein	2.41	26.76		
15E	n3 vein	2.10	17.30		
15E	n3 vein (infill)	3.08	25.63		
18	n3 vein	2.80	20.56		
18_2	n3 vein (infill)	2.63	23.38		
0606	s2 vein	2.13	27.25		
w03a	n3 vein	3.05	22.71		
w03a	n3 vein	3.00	24.84		
wn01	n3 vein	2.09	27.67		
0606	n3 vein	2.62	20.77		
0609	n3 vein	1.58	21.26		
e03	n3 breccia	3.05	27.18		
e07	n3 vein	3.05	26.85	0.99	1.01
e07	matrix (frag.)	3.08	26.56		
e07	n3 breccia	0.80	26.87	0.26	1.01
0607c	**zebra vein**	**3.36**	**26.12**	**1.01**	**1.01**
0607c	**matrix**	**3.33**	**25.82**		
wn04	v1 vein	1.37	27.59		

v1: first generation veins perpendicular to the bedding.
s2: veins associated with bedding-parallel shear.
n3: veins associated with normal faulting.
n3 (infill): brownish discolored material in fault cement.
[a] Matrix values of the upper0607 sample used to calculate the ratio.

the regular arrangement of the fragments into the sub-parallel bands (Renard et al., 2005).

A single event here formed a single, or a few 10–50 μm wide fractures simultaneously. These fractures were required to heal until further fracturing occurred in order to avoid the collapse and gravitational transport of fragments. The location of the fractures is marked by sub-parallel host rock flakes within the vein bundles. Similar to the structures described by Renard et al. (2005), the apertures of the individual veinlets appear to be approximately constant (Figs. 5 and 7). On the contrary the anastomosing pattern and bundling of the structures lead to the impression of a self-similar system (Fig. 6).

The individual veinlets show irregular shapes, or trajectories, and do not exhibit any evidence for cross-cutting. For this reason we interpret them to have formed in a subcritical mode.

We conclude that the formation of the zebra texture was related to the mechanical properties of the vein's cement: all our observations indicate a constant restoration of strength across the fracture. The veinlets are trans-granular, suggesting that, until new veinlets were formed, the matrix was already consolidated. The

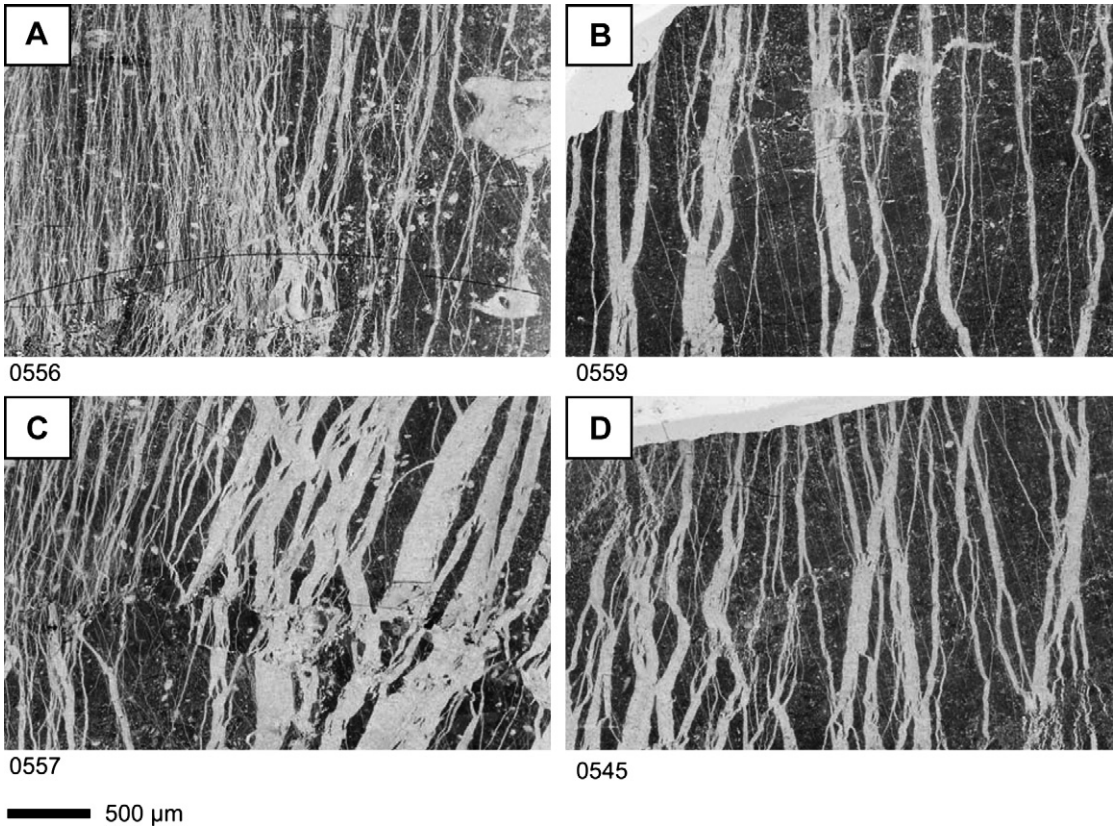

Fig. 5. Scanned thin sections of selected samples show a dense vein network of the zebra textures. The veins show an anastomosing geometry with intense branching (all samples from Location 83; scale bar is 5 mm; histogram stretch applied).

veinlets show an affinity to curve towards or merge with the vein bundles and to interact with the vein/matrix interface. The veinlets only seldom cross-cut each other, suggesting the vein's cement to be strong. On the other hand, the interface between the vein and the matrix must have had sufficient strength to allow host rock fragments to fail rather than breaking the bond of the interface itself.

3.1. Formation of the vein network

In what follows, we present a simple model to explain the formation of the vein network in a dynamic system of multiple crack–seal events.

3.1.1. Cementation of the network

We interpret the cementation cycle to be made up of the following stages:

(1) Individual cement grains grow to sizes much larger than the individual veinlets in extreme growth competition (possibly starting from sparse nucleation sites) after the formation of a fracture (Fig. 9B and C). The crystals grew within an open void (Cox and Etheridge, 1983; Hilgers et al., 2004; Nollet et al., 2006). (2) Large parts of the fracture are healed prior to a new fracture event (Fig. 9D). (3) Renewed failure does not occur within the vein (Fig. 9E), but adjacent to it, as the newly formed vein is stronger than the matrix (Woodcock et al., 2007). The new fracture may cut/touch the cement of the previous veinlet, as well as the matrix, with a sub-parallel trajectory. (4) The growth competition continues (Fig. 9F) and reseals the newly formed fracture (Fig. 9G). This kind of growth competition allows individual cement grains to grow laterally, and into different branches, within a crack–seal system.

3.1.2. Mechanical properties of crack–seal systems

We now ask the question: what controls the location of the next fracture after the sealing of a previous one? The pattern created by successive fracture and sealing events is illustrated by the following model.

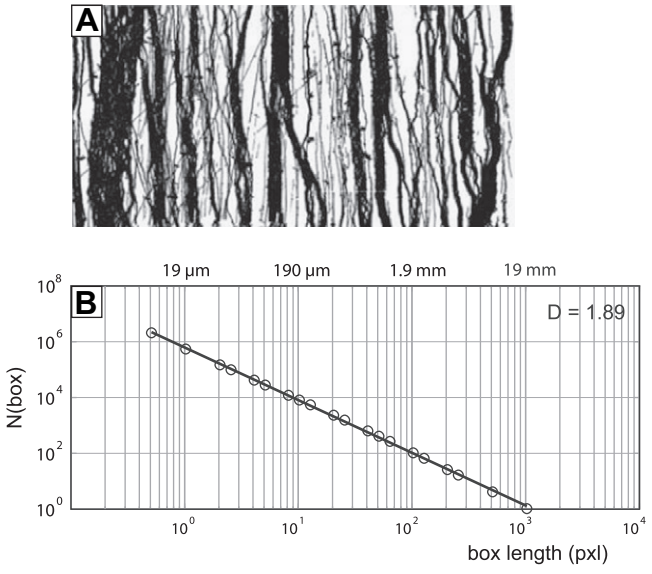

Fig. 6. Box-counting results on the fractal dimension of the vein pattern of sample 0563 shown in Fig. 7b. A binary image (A) obtained by a threshold filter applied to the thin section (2048 × 1024 pxl.) was analyzed with a box-counting algorithm using 20 different integer box sizes. The box-counting curve (B) shows an approximately linear relationship with a fractal dimension of $D = 1.89$. True dimensions are given on the upper axis.

The location and trajectory of the newly formed fractures are interpreted to be affected by two factors: (i) The ratio between the strengths of cement, matrix and interface, and (ii) the distribution, or heterogeneity, of these material properties in the system.

3.1.2.1. Effects of different strength ratios of matrix, cement, and interface. The three mechanical components of a crack–seal system are: (i) The matrix (M), which we assume for our model to be isotropic and homogeneous, (ii) the vein's cement (C), and (iii) the interface (I) between the matrix and cement.

Differences in the tensile strength (T) of the three components impact the geometry of the system during successive crack–seal events, as illustrated by five examples in Fig. 10.

If the vein's cement is the weakest element ($T_C < T_I$, T_M), the formation of new veinlets is likely to be focused on the first existing vein (Fig. 10, case 1) (Fig. 8 in Urai et al., 1991). The location of the newly formed fractures in the preexisting vein is not well defined because the material properties are the same ($T_{C(n+1)} = T_{C(n)}$). Successive events in such conditions will form stretched crystals.

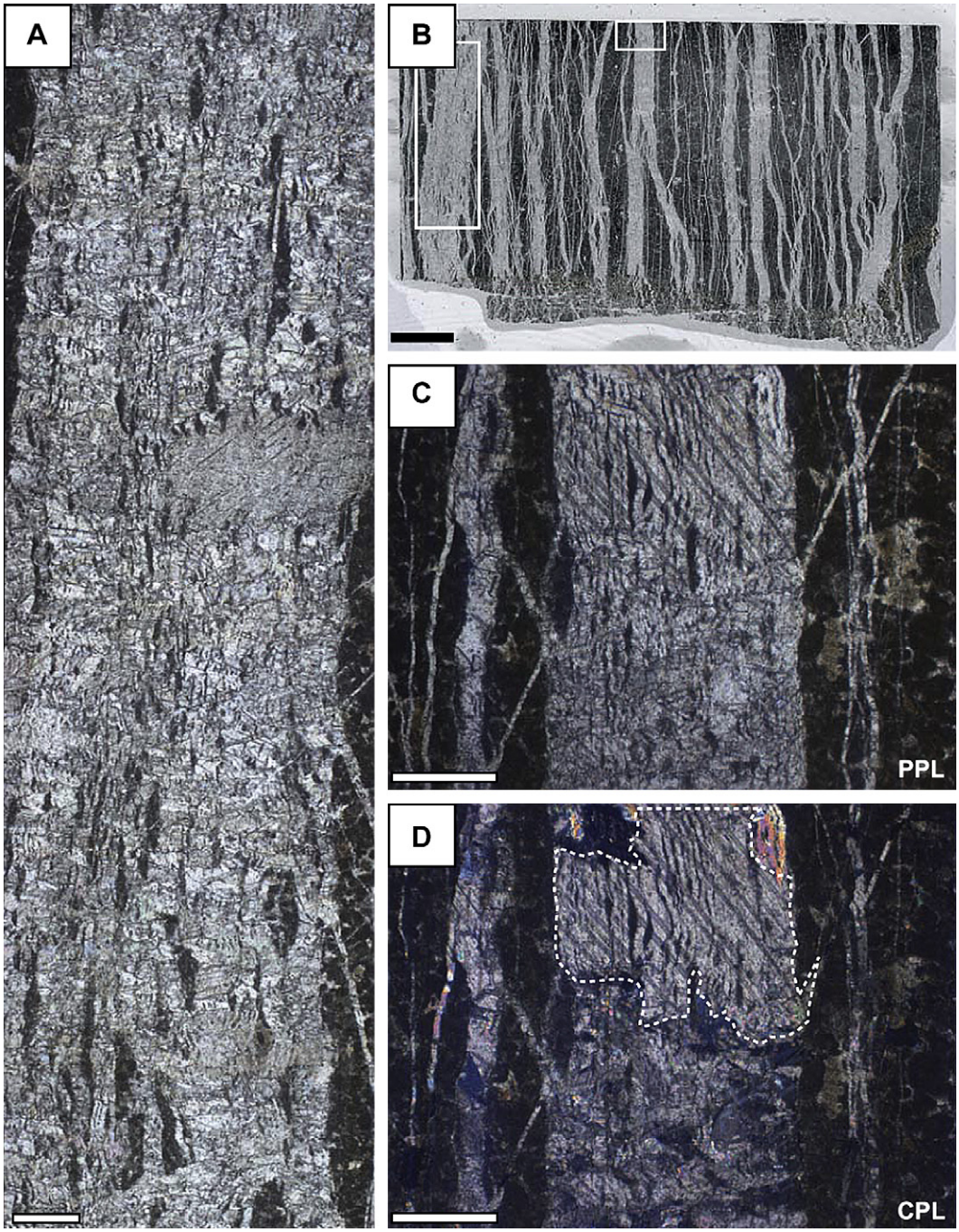

Fig. 7. Subsets and overview of the thin section 0563 from Location 83. (A) The vertical vein shows multiple inclusions of the wall rock material. Scale bar is 500 μm, plain light. (B) Overview of the thin section with a dense vein network; boxes show the location of the subsets. Scale bar is 5 mm, plain light. (C) Subset of the thin section observed with parallel polarizer. The vein consists of multiple parallel segments visible by inclusions of wall rock material. (D) Crossed polarizer of previous image shows that grains span several generations of wall rock inclusions. Scale bar is 500 μm.

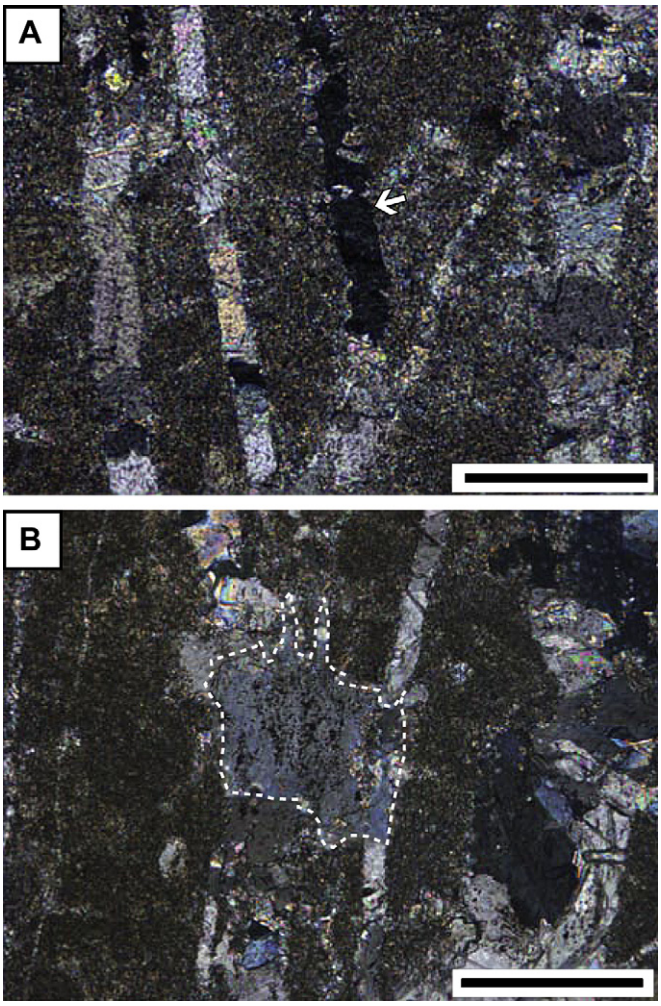

Fig. 8. (A) Thin section image with CPL showing the wide lateral extents of single calcite grains (arrow). (B) Thin section image with CPL of a large calcite grain (dotted) spanning several veinlets. Sample 0563; all scale bars are 200 μm.

The opposite applies if the matrix is much weaker than the interface or the cement (Fig. 10, case 2, $T_M < T_C$, T_I). In this case the fracturing is mainly focused within the matrix (Lee and Wiltschko, 2000; Woodcock et al., 2007). The veinlets within such a system rarely cross-cut each other, and a sub-parallel but random pattern develops.

Extensive cross-cutting is expected when the strength of the elements is approximately the same (Fig. 10, case 3, $T_c = T_I = T_M$). A random pattern evolves, as the material strength is continuously restored in a homogenous manner.

If however the strength of one element deviates slightly from the others, an anastomosing and branching pattern is expected. When the cement is slightly stronger than the other elements (Fig. 10, case 4, $T_c \geq T_I$, T_M), the veinlets form preferentially in the matrix, or along the interfaces, rarely cross-cutting the slightly stronger veins. Fractures that propagate obliquely towards a vein are likely to curve and touch the interface in sub-parallel trajectory forming an anastomosing pattern. Branching is common because of the strength similarities of the three materials. Depending on which element is the strongest, the affinity of the veinlets changes to form either in the matrix, along the interfaces, or within the veins.

A fifth case is imaginable, in which the strength of the interface is significantly smaller than the other two materials (Fig. 10, case 5, $T_I < T_C$, T_M). In this case (e.g. a different mineral phase within antitaxial veins (e.g. Cox, 1987; Renard et al., 2005; Urai et al., 1991)) failure is localized in the interface thus leading to parallel inclusion bands. Based on this model, the observed zebra patterns with a prominent anastomosing pattern fall somewhere between cases 2 and 4, with the veins preferentially forming in the matrix and along the interfaces. The higher strength of the cement prevents the cross-cutting of the veinlets, while the similar strengths of matrix and interfaces lead to the braided network observed in the zebra patterns.

3.1.2.2. Cement distribution or lateral distribution of strength. Another explanation for the formation of the anastomosing pattern could be an incomplete healing, which leads to lateral changes in the strength of the interface between vein and matrix (Henderson et al., 1990). Healing of a fracture within a growth competition environment, or sparse nucleation sites, causes a laterally heterogeneous strength distribution, as closed sections in the fracture coexist with open ones over a long period of time. This is in contrast to a fracture sealed without these factors (Fig. 11) in which an equally progressing growth front closes and seals the fracture more evenly.

The average opening of a fracture in our samples is in the order of 10–50 μm only. With the proposed growth processes the growth front of the cement is not parallel to the fracture wall. As a few individual grains locally seal the fracture, the growth front spreads laterally (Figs. 11A and 12B–D). From early stages onwards, sealed parts coexist with unsealed parts. This is very different to a system in which the fracture is closed evenly along its length by a growth front parallel to its walls (Nollet et al., 2006) (Fig. 11B). The latter case (Fig. 11B) shows similar mechanical conditions along the entire fracture over a long period of time, until the cement fronts touch each other at later stages. However, according to the growth competition observed in the zebra patterns, some parts of the fracture could have been effectively healed while others remained open (Fig. 12D, Henderson et al., 1990). This would lead to heterogeneous mechanical properties along the fracture surface. If renewed failure occurs prior to the complete healing of the fracture, the open sections (or areas of low-bond strength) will presumably dictate the trajectory of a new fracture (Fig. 12E).

3.1.3. Timing of failure

Based on our observations it seems clear that the studied fractures were partly or completely healed prior to a successive fracturing event. This conclusion suggests that the healing process (the growth of cement crystals) is faster than the deformation rate which could potentially rupture the healing vein (Fig. 13 in Hilgers et al., 2001). Within a crack–seal cycle, the system shows the lowest strength with the crack formation. At this stage, the fracture will localize any strain. Such localization is however not observed, as the apertures of the individual zebra veinlets are approximately the same and distributed. This means that localized strain must have halted until the mechanical strength of the system was restored. A possible explanation for this behavior could be a cyclic fluid-pressure build-up and release that occurs in the very proximity of the newly formed fracture as a result of its own formation (Henderson et al., 1990; Petit et al., 1999; Townend and Zoback, 2000).

Similar to the crack–seal textures described and discussed by Renard et al. (2005), we interpret this supersaturated vein network to have formed within a constant remote stress field rather than being caused by events of different magnitudes (e.g. earthquakes), which could explain the similar veinlet apertures. We interpret the large amount of individual veinlets to have

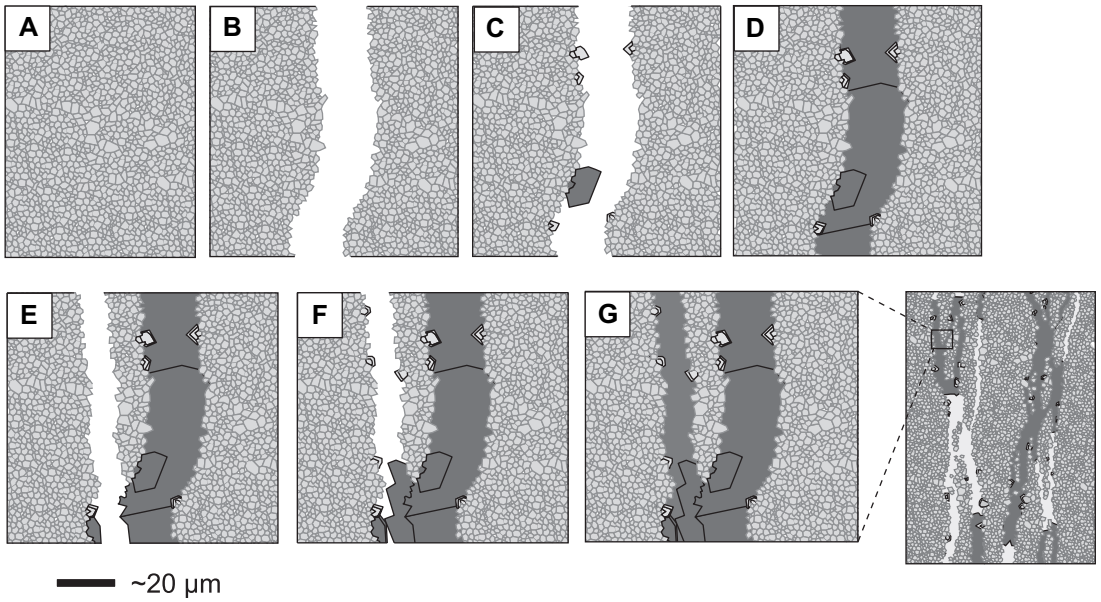

Fig. 9. Conceptional model for the formation of the zebra pattern. An intact section of rock (A) forms a single fracture (B). Within the fracture (C) nucleation of calcite crystals occurs on the fracture walls. In an extreme growth competition, a few crystal grains prevail within the cement marked by dark gray (D). Renewed fracturing may rupture the previous veinlet (E), so that the growth competition starts again (F). This process (G) could explain that single cement grains extend into numerous branches of the vein network (simplified model; not to scale).

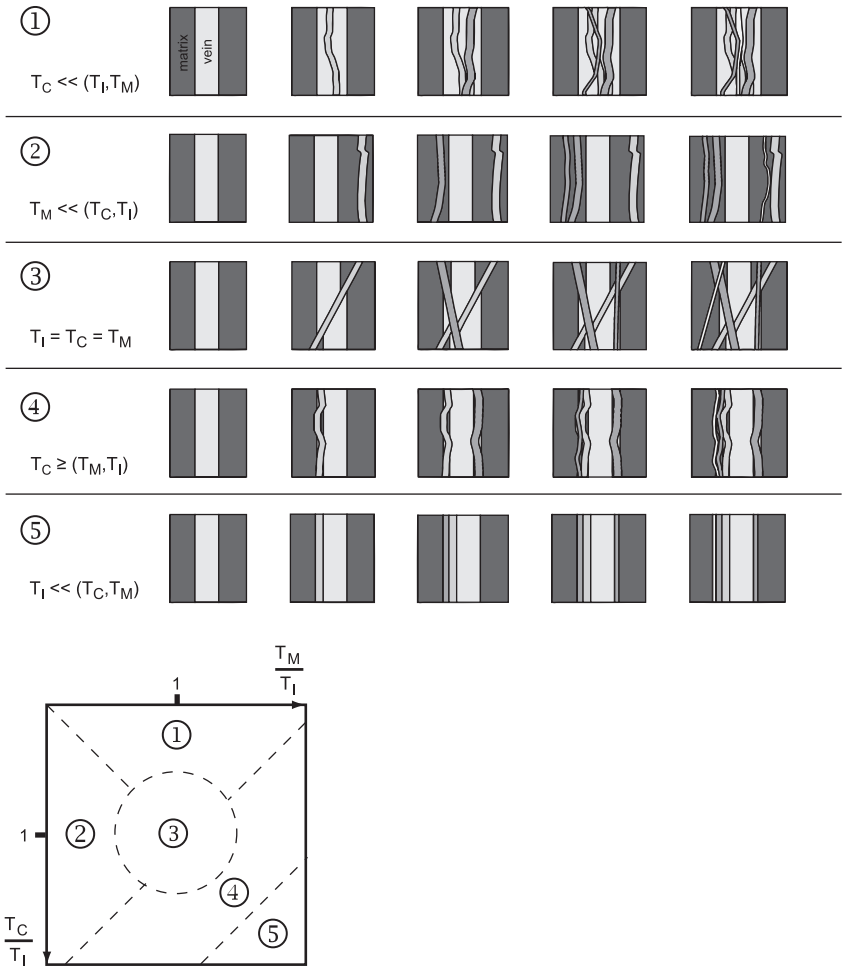

Fig. 10. Conceptional model on the impact of the mechanical strength of matrix (T_M), vein cement (T_C) and the interface (T_I) on the formation of successive fracture and healing events. Cases 1–5 are explained in the text and represent successive stages (simplified model; not to scale).

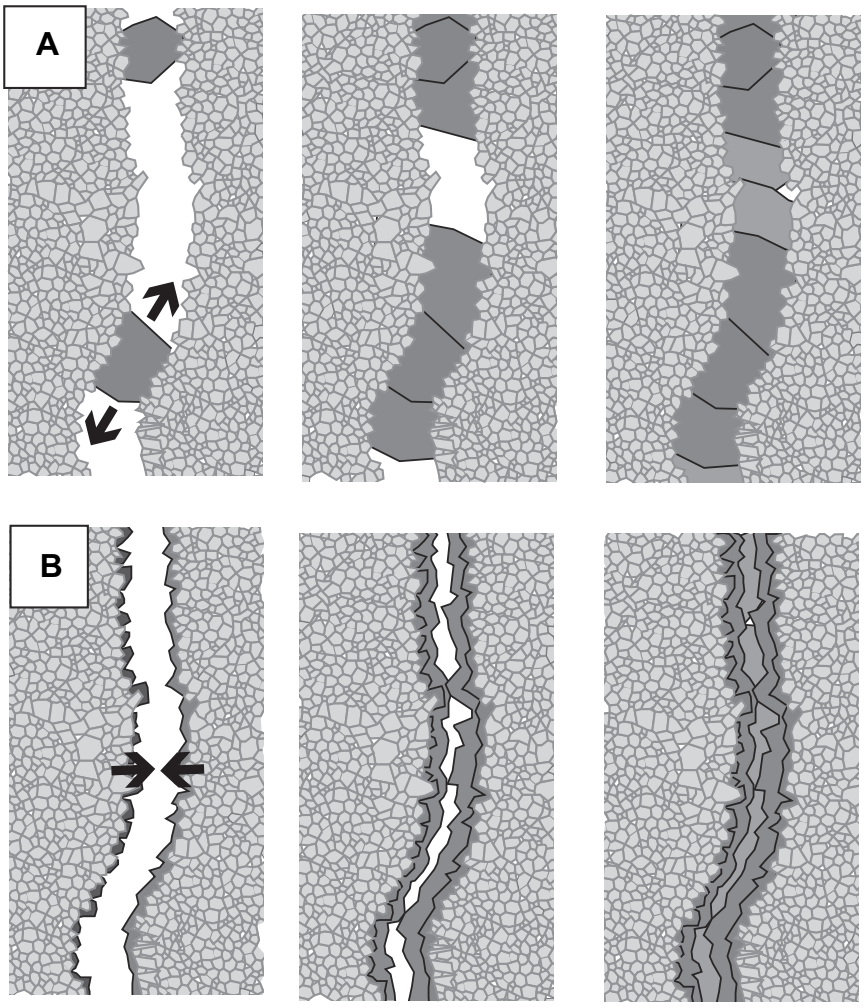

Fig. 11. Conceptional model on the cementation of a fracture with extreme growth competition (A) and without extreme growth competition (B). Note that with the growth competition the fracture is quickly healed at isolated locations. The cementation then spreads laterally increasing the mechanical strength. Until complete healing, a heterogeneous strength distribution is apparent. Without the extreme growth competition the fracture is evenly cemented. Mechanical healing occurs at a much later stage (simplified model; not to scale).

formed in a cyclic system fluid-pressure variations in a small-scale self-sealing system (Cowie, 1998; Petit et al., 1999; Townend and Zoback, 2000).

4. Conclusion

The zebra textures described in this study are interpreted as an anastomosing crack–seal pattern forming patches of extremely high density (supersaturated) vein networks. The applied analysis (EDX, cathodoluminescence, stable isotopes and staining with Alizarin and potassium ferricyanide) showed no indications for chemical zonation, suggesting a homogenous, presumably rock-buffered system. The governing processes are characterized by the growth of a few calcite grains within a veinlet, which seal it over large distances. The process creating such grains can either be extreme growth competition or the sparse distribution of nucleation sites along the fractures. Both these mechanisms lead to an effective, but intermittent, healing of newly formed fractures. Localization to a single fracture is prevented by sealing with strong calcite cement. It is unclear if the period of healing between successive fracturing events is related to a fluid-pressure drop with the formation of a fracture. In such a case, zebras could document a continuous feed-back system of cyclic crack–seal and pressure build-up and release events. The anastomosing pattern itself is interpreted to be a result of the mechanical properties of cement, interface, and matrix. The textures observed and the models presented in this study are 2D representations. It is unclear what the zebra textures look like in 3D, and how fluid flow conduits evolve within such a self-sealing system. Although the formation of the vein network is interpreted to be the result of numerous fracturing events, the connection of the zebra patches and the adjacent massive veins raises the question of the larger scale bulk permeability and strength of this system.

Acknowledgements

We would like to thank Johannes Schoenherr for assistance during fieldwork and the help with the micro-structural analyses. Werner Kraus and Philipp Binger processed the samples for the micro-structural work. We like to thank Uwe Wollenberg from the Geological Institute RWTH Aachen University for his assistance in the cathodoluminescence and SEM work. Critical reviews by Anne-Marie Boullier and an anonymous reviewer significantly improved the manuscript and made us aware of the role of sparse nucleation sites. Additional comments by the editor and his team are greatly acknowledged.

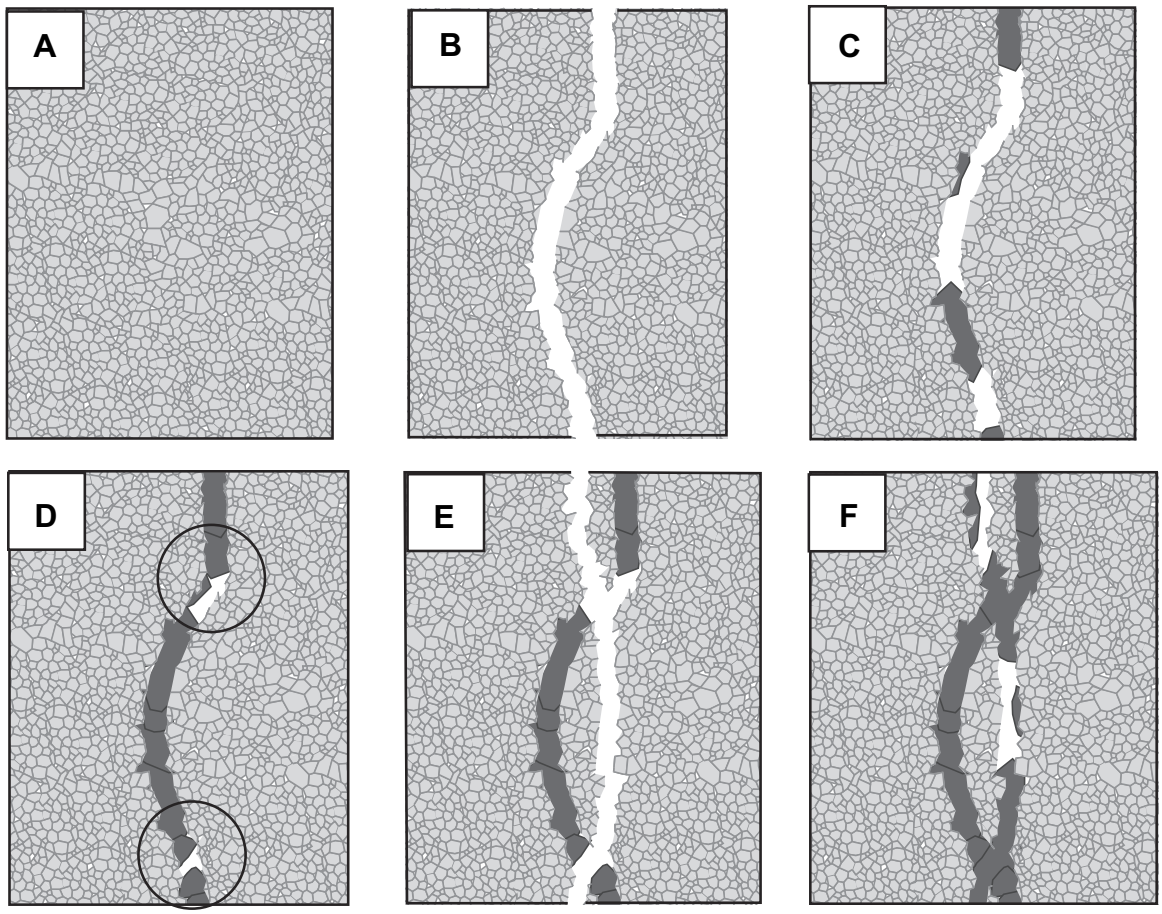

Fig. 12. A possible explanation for the sub-parallel anastomosing network of veinlets is related to the lateral growth of cement crystals. With formation of a fracture in the material (A, B), the proposed growth competition leads to rapid cementation of the fracture. The cement grains quickly seal parts of the fracture (C) leading to effective local bonds, while other parts of the fracture remain unsealed. With prolonged cementation (D), the grains grow laterally filling the fracture, increasing the strength of the system. If rupture sets in before the fracture plane is entirely cemented, uncemented areas (circles) may dictate the trajectory of the newly formed fracture (E). Repeating this process (F) could form a supersaturated anastomosing network of veinlets (simplified model; not to scale).

References

Adams, A.E., MacKenzie, W.S., 2001. A Colour Atlas of Carbonate Sediments and Rocks Under The Microscope. Manson Publishing Ltd., London.

Al-Wardi, M., 2006. Structural Evolution of the Jebel Akhdar Culmination and its Implications for Exhumation Processes in the Northern Oman Mountains. University of Leeds.

Al-Wardi, M., Butler, R.W.H., 2006. Constrictional extensional tectonics in the northern Oman Mountains, its role in culmination development and the exhumation of the subducted Arabian margin. In: Ries, A.C., Butler, R.W.H., Graham, R.H. (Eds.), Deformation of the Continental Crust: the Legacy of Mike Coward. Geological Society of London Special Publications, vol. 272, pp. 187–202.

Andreani, M., Baronnet, A., Boullier, A.M., Gratier, J.P., 2004. A microstructural study of a "crack–seal" type serpentine vein using SEM and TEM techniques. European Journal of Mineralogy 16, 585–595.

Badoux, V., Moritz, R., Fontbote, L., 2001. The Mississippi Valley-type Zn–Pb deposit of San Vicente, Central Peru: an Andean syntectonic deposit. In: Piestrzynski, A. (Ed.), Mineral Deposits at the Beginning of the 21st Century. Balkema, Amsterdam, pp. 191–195.

Beurrier, M., Bechennec, F., Hutin, G., Rabu, D., 1986. Rustaq, Geological Map Oman 1:100,000; Sheet NF40-3D. Ministry of Petroleum and Minerals, Sultanate of Oman.

Boullier, A.M., Robert, F., 1992. Paleoseismic events recorded in Archean gold–quartz vein networks, Val d'Or, Abitibi, Canada. Journal of Structural Geology 14 (2), 161–179.

Breton, J.P., Béchennec, F., Le Métour, J., Moen-Maurel, L., Razin, P., 2004. Eoalpine (Cretaceous) evolution of the Oman Tethyan continental margin: insights from a structural field study in Jabal Akhdar (Oman mountains). GeoArabia 9 (2), 1–18.

Cowie, P.A., 1998. A healing–reloading feedback control on the growth rate of seismogenic faults. Journal of Structural Geology 20 (8), 1075–1087.

Cox, S.F., 1987. Antitaxial crack–seal vein microstuctures and their relationship to displacement paths. Journal of Structural Geology 9 (7), 779–787.

Cox, S.F., Etheridge, M.A., 1983. Crack–seal fibre growth mechanisms and their significance in the development of oriented layer silicate microstructures. Tectonophysics 92, 147–170.

El-Shazly, A.K., Bröcker, M., Hacker, B., Calvert, A., 2001. Formation and exhumation of blueshists and eclogites from NE Oman: new perspectives from Rb-SR and 40Ar/39Ar dating. Journal of Metamorphic Geology 19, 233–248.

Filbrandt, J.B., Al-Dhahab, S., Al-Habsy, A., Harris, K., Keating, J., Al-Mahruqi, S., Ozkaya, S.I., Richard, P.D., Robertson, T., 2006. Kinematic interpretation and structural evolution of North Oman, Block 6, since the Late Cretaceous and implications for timing of hydrocarbon migration into Cretaceous reservoirs. GeoArabia 11 (1), 97–140.

Gaviglio, P., 1986. Crack–seal mechanism in limestone: a factor of deformation in strike-slip faulting. Tectonophysics 131, 247–255.

Glennie, K.W., 2005. The Geology of the Oman Mountains – an Outline of Their Origin. Scientific Press Ltd.

Gray, D.R., Gregory, R.T., Amstrong, R.A., Richards, I.J., Miller, J.M., 2005a. Age and stratigraphic relationships of structurally deepest level rocks, Oman Mountains: U/Pb SHRIMP evidence for Late Carboniferous Neothethys rifting. The Journal of Geology 113 (6), 611–626.

Gray, D.R., Gregory, R.T., Miller, J.M., 2005b. Comment on "Structural evolution, metamorphism and restoration of the Arabian continental margin, Saih Hatat region, Oman Mountains" by M.P. Searle et al. Journal of Structural Geology 27, 371–374.

Gray, D.R., Miller, J.M., 2000. A new structural profile along the Muscat–Ibra transect, Oman: implications for emplacement of the Samail ophiolite. In: Dilek, Y., Moores, E.M., Elthon, D., Nicolas, A. (Eds.), Ophiolites and Oceanic Crust: New Insights from Field Studies and the Ocean Drilling Programme. Geological Society, America, Special Publications, vol. 349, pp. 513–523.

Henderson, J.R., Henderson, M.N., Wright, T.O., 1990. Water–sill hypothesis for the origin of certain veins in the Meguma Group, Nova Scotia, Canada. Geology 18 (7), 654–657.

Hilgers, C., Dilg-Gruschinski, K., Urai, J.L., 2004. Microstructural evolution of syntaxial veins formed by advective flow. Geology 32 (3), 261–264.

Hilgers, C., Kirschner, D.L., Breton, J.P., Urai, J.L., 2006. Fracture sealing in a regional, high-pressure cell in Jabal Akhdar, Oman mountains – first results. Geofluids 6 (2).
Hilgers, C., Koehn, D., Bons, P.D., Urai, J.L., 2001. Developent of crystal morphology during unitaxial growth in a progressively widening vein: II. Numerical simulations of the evolution of antitaxial fibrous veins. Journal of Structural Geology 23, 873–885.
Hilgers, C., Urai, J.L., 2005. On the arrangement of solid inclusions in fibrous veins and the role of the crack–seal mechanism. Journal of Structural Geology 27 (3), 481–494.
Marc Holland, Janos L. Urai, Philippe Muchez and Emanuel J.M. Willemse (2009), Evolution of fractures in a highly dynamic, thermal, hydraulic, and mechanical system - (I) Field observations in Mesozoic Carbonates, Jabal Shams, Oman Mountains, GeoArabia, vol. 14, No. 1, p.57–110.
Marc Holland, Nishank Saxena and Janos L. Urai (in press), Evolution of fractures in a highly dynamic thermal, hydraulic, and mechanical system - (II) Remote sensing fracture analysis, Jabal Shams, Oman Mountains, GeoArabia, v. 14, No. 3, 2009, p. 163-194.
Hughes Clarke, M.W., 1988. Stratigraphy and rock unit nomenclature in the oil-producing area of interior Oman. Journal of Petroleum Geology 11 (1), 5–60.
Kraus, W., 2002a. ATP Reagenz und Lamipeel. Der Präparator 48 (2), 51–75.
Kraus, W., 2002b. Lamipeel-Präparation: Eine neue effiziente Methode zur Strukturdokumentation von Karbonat-Bohrkernproben. Mitt. Ing. u. Hydrogeol., 80.
Kusky, T., Robinson, C., El-Baz, F., 2005. Tertiary–Quaternary faulting and uplift in the northern Oman Hajar Mountains. Journal of the Geological Society 162 (5), 871–888.
Lee, Y.J.Y.J., Wiltschko, D.V., 2000. Fault controlled sequential vein dilation: competition between slip and precipitation rates in the Austin Chalk, Texas. Journal of Structural Geology 22 (9), 1247–1260.
Loosveld, R.J.H., Bell, A., Terken, J.J.M., 1996. The tectonic evolution of interior Oman. GeoArabia 1 (1), 28–51.
Merino, E., Canals, À, Fletcher, R.C., 2006. Genesis of self-organized zebra textures in burial dolomites: displacive veins, induced stress, and dolomitization. Geologica Acta 4 (3), 383–393.
Nielsen, P., Flipkens, V., Groessens, E., Swennen, R., 2000. Sedimentology and diagenesis of the Dinantian succession in the Vinalmont Borehole. Geologica Belgica 3 (3–4), 369–393.
Nielsen, P., Swennen, R., Muchez, P., Keppens, E., 1998. Origin of Dinantian zebra dolomites south of the Brabant–Wales Massif, Belgium. Sedimentology 45, 737–743.
Nollet, S., Hilgers, C., Urai, J.L., 2006. Experimental study of polycrystal growth from an advecting supersaturated fluid in a model fracture. Geofluids 6, 185–200.
Nollet, S., Urai, J.L., Bons, P.D., Hilgers, C., 2005. Numerical simulations of polycrystal growth in veins. Journal of Structural Geology 27 (2), 217–230.
Patton, T.L., O'Conner, S., 1988. Cretaceous flexural history of the northern Oman Mountains foredeep, United Arab Emirates. Bulletin of American Association of Petroleum Geologists 72, 797–807.
Petit, J.P., Wibberley, C.A.J., Ruiz, G., 1999. 'Crack–seal', slip: a new fault valve mechanism? Journal of Structural Geology 21 (8–9), 1199–1207.
Ramsay, J.G., 1980. The crack–seal mechanism of rock deformation. Nature 284 (5752), 135–139.
Renard, F., Andreani, M., Boullier, A.M., Labaume, P., 2005. Crack–seal patterns; records of uncorrelated stress release variations in crustal rocks. In: Gapais, D., Brun, J.P., Cobbold, P.R. (Eds.), Deformation, Mechanisms, Rheology and Tectonics: From Mineral to the Lithosphere. Geological Society, London, Special Publications, vol. 243, pp. 67–79. United Kingdom.
Searle, M.P., 2007. Structural geometry, style and timing of deformation in the Hawasina Window, Al Jabal al Akhdar and Saih Hatat culminations, Oman Mountains. GeoArabia 12 (2), 99–130.
Searle, M.P., 2007. Structural geometry, style and timing of deformation in the Hawasina Window, Al Jabal al Akhdar and Saih Hatat culminations, Oman Mountains. GeoArabia 12 (2), 99–130.
Searle, M.P., Warren, C.J., Parrish, R.R., 2005. Reply to: Comment by Gray, Gregory and Miller on "Structural evolution, metamorphism and restoration of the Arabian continental margin, Saih Hatat region, Oman Mountains". Journal of Structural Geology 27, 375–377.
Swennen, R.A.J., Vandeginste, V., Ellam, R., 2003. Genesis of zebra dolomites (Cathedral formation; Canadian Cordillera fold and thrust belt, British Columbia). Journal of Geochemical Exploration 78–79, 571–577.
Townend, J., Zoback, M.D., 2000. How faulting keeps the crust strong. Geology 28 (5), 399–402.
Urai, J.L., Williams, P.F., van Roermund, H.L.M., 1991. Kinematics of crystal growth in syntectonic fibrous veins. Journal of Structural Geology 13 (7), 823–836.
Vandeginste, V., Swennen, R., Gleeson, S.A., Ellam, R.M., Osadetz, K., Roure, F., 2005. Zebra dolomitization as a result of focused fluid flow in the Rocky Mountains Fold and Thrust Belt, Canada. Sedimentology 52 (5), 1067–1095.
Walsh, J.J., Watterson, J., 1993. Fractal analysis of fracture patterns using the standard box-counting technique: valid and invalid methodologies. Journal of Structural Geology 15 (12), 1509–1512.
Warbuton, J., Burnhill, T.J., Graham, R.H., Isaac, K.P., 1990. The evolution of the Oman Mountains foreland basin. In: Robertson, A.H.F., Searle, M.P., Ries, A.C. (Eds.), The Geology and Tectonics of the Oman Region. Geological Society, London, Special Publication No. 49, pp. 419–427.
Warren, C.J., Miller, J.M., 2007. Structural and stratigraphic controls on the origin and tectonic history of a subducted continental margin, Oman. Journal of Structural Geology 29, 541–558.
Warren, C.J., Parrish, R.R., Searle, M.P., Waters, D.J., 2003. Dating the subduction of the Arabian continental margin beneath the Semail ophiolite. Oman. Geology 31 (10), 889–892.
Weller, H., 1989. Sedimentologie von Mud Mounds und ihr Nachweis im Harz. Wiss. Z. Ernst-Moritz-Arndt-Univ. Greifswald. Math.nat.wiss. Reihe 38 (1–2), 70–78.
Wilson, H.H., 2000. The age of the Hawasina and other problems of Oman Mountain Geology. Journal of Petroleum Geology 23 (3), 345–362.
Wiltschko, D.V., Morse, J.W., 2001. Crystallization pressure versus "crack seal" as the mechanism for banded veins. Geology 29 (1), 79–82.
Woodcock, N.H., Dickson, J.A.D., Tarasewicz, J.P.T., 2007. Transient permeability and reseal hardening in fault zones: evidence from dilation breccia textures. In: Geological Society, London, Special Publications, vol. 270, pp. 43–53.